A Model-Based fMRI Analysis With Hierarchical Bayesian Parameter Estimation

Woo-Young Ahn, Adam Krawitz, Woojae Kim, Jerome R. Busemeyer, and Joshua W. Brown
Indiana University Bloomington

A recent trend in decision neuroscience is the use of model-based functional magnetic resonance imaging (fMRI) using mathematical models of cognitive processes. However, most previous model-based fMRI studies have ignored individual differences because of the challenge of obtaining reliable parameter estimates for individual participants. Meanwhile, previous cognitive science studies have demonstrated that hierarchical Bayesian analysis is useful for obtaining reliable parameter estimates in cognitive models while allowing for individual differences. Here we demonstrate the application of hierarchical Bayesian parameter estimation to model-based fMRI using the example of decision making in the Iowa Gambling Task. First, we used a simulation study to demonstrate that hierarchical Bayesian analysis outperforms conventional (individual- or group-level) maximum likelihood estimation in recovering true parameters. Then we performed model-based fMRI analyses on experimental data to examine how the fMRI results depend on the estimation method.

Keywords: model-based fMRI, functional magnetic resonance imaging, reinforcement learning, hierarchical Bayesian analysis, model comparison

How we make decisions to obtain rewards and avoid punishments is a fundamental topic across research areas including psychology, economics, neuroscience, and computer science. In the past decade, decision neuroscience researchers have begun to approach decision making from an interdisciplinary perspective—integrating quantitative models with neural signals. For example, early pioneering studies demonstrated that the phasic responses of midbrain dopamine neurons can be well described by the temporal-difference reinforcement learning algorithm (Montague, Dayan, & Sejnowski, 1996; Schultz, Dayan, & Montague, 1997). More recently, human functional magnetic resonance imaging (fMRI) studies have shown that blood-oxygen-level-dependent (BOLD) activations in brain regions including the striatum and orbitofrontal cortex correlate with prediction error signals from the temporal-difference learning model (McClure, Berns, & Montague, 2003; O'Doherty, Dayan, Friston, Critchley, & Dolan, 2003). These fMRI studies used the method of "model-based fMRI," in which a mathematical model of behavior provides a framework to study neural mechanisms of reward learning. In model-based fMRI, predictions derived from a mathematical model of choice behavior are correlated with fMRI data to determine brain areas related to postulated decision-making processes. This method is increasingly popular in decision neuroscience because it provides insight into the neural correlates of predicted cognitive processes and can be useful to discriminate competing theories of brain function (see O'Doherty, Hampton, & Kim, 2007, for a review and methodological recipe).

The first step in model-based fMRI is to estimate the free parameters in the mathematical model of behavior. Getting accurate parameter estimates is important not only because parameter estimates reflect psychological traits (e.g., the learning rate or the balance of exploitation

Woo-Young Ahn, Adam Krawitz, Woojae Kim, Jerome R. Busemeyer, and Joshua W. Brown, Department of Psychological and Brain Sciences, Indiana University Bloomington.

Adam Krawitz is now at Department of Psychology, University of Victoria, Victoria, Canada.

Correspondence concerning this article should be addressed to Joshua W. Brown, Department of Psychological and Brain Sciences, 1101 East 10th Street, Indiana University, Bloomington, IN 47405. E-mail: jwmbrown@indiana.edu

and exploration), but also because they affect the results of the subsequent model-based fMRI analysis (e.g., Tanaka et al., 2004). Most previous studies with model-based fMRI have used group-level analysis with maximum likelihood estimation (MLE). In group-level analysis, free parameters are assumed to be homogenous across participants and no individual differences are taken into account. It might be tolerable to ignore individual differences in simple conditioning tasks where most participants behave similarly, but it is inappropriate in complex tasks where substantial individual differences exist. To take into account individual differences, an alternative approach is individual-level analysis. However, using MLE for individual-level analysis can lead to noisy and unreliable estimates if the amount of information from each individual is limited, as is often the case in neuroimaging studies. We propose the use of hierarchical Bayesian analysis (HBA) to reconcile the tension between individual differences and reliable parameter estimation.

HBA is an advanced branch of Bayesian statistics (Berger, 1985) that uses the basic principles of Bayesian statistical inference (Gelman, Carlin, Stern, & Rubin, 2004). One of the advantages of HBA is that, whereas MLE finds a point estimate for each parameter that maximizes the likelihood of the data, HBA finds a full posterior distribution of belief across the range of values a parameter can take on. A second advantage of HBA is that it allows for individual differences while pooling information across individuals in a coherent way. Both individual and group parameter estimates are found simultaneously in a mutually constraining fashion. By capturing the commonalities among individuals, each individual's parameter estimates tend to be more stable and reliable because they are informed by the group tendencies.

In this article, we apply HBA to model-based fMRI analysis of the Iowa Gambling Task (IGT; Bechara, Damasio, Damasio, & Anderson, 1994) and compare it with other estimation methods. The remainder of this article is organized as follows. First, we briefly explain the IGT and a mathematical model for the task. Second, we briefly explain the procedures of MLE and HBA and then use simulated data with known true parameter values to examine which method recovers the values more accu-

rately. To tease apart the relative contributions of Bayesian estimation and the use of a hierarchical approach, we estimate parameters using each of the following methods: MLE at the group level (MLE-Group), MLE at the individual level (MLE-Ind), nonhierarchical Bayesian analysis (Bayes-Ind), and HBA. Third, we present model-based fMRI analyses using parameter estimates from MLE-Group, MLE-Ind, and HBA and show how the choice of method influences the fMRI results.

IGT

The IGT is a well-established task used to study decision-making processes in control participants and decision-making deficits in clinical populations including substance abusers and patients with brain lesions (Bechara, Damasio, Tranel, & Damasio, 1997; Bechara et al., 2001). The goal of the task is to maximize monetary gains while repeatedly choosing cards from one of four decks. Each selection results in a monetary gain, draw, or loss. There are two "good" decks with long-term gains and two "bad" decks with long-term losses. However, the typical win is larger for the bad decks than the good decks, putting the magnitude of the potential immediate gain into opposition with the long-term cumulative outcome from the decks. Furthermore, one bad deck and one good deck have infrequent larger losses, and the other bad and one good deck have more frequent smaller losses. Participants need to learn from experience which decks are advantageous for good performance. It is a challenging task and even healthy control participants show substantial individual differences in behavioral performance.

Prospect Valence Learning (PVL) Model

We used the PVL model (Ahn, Busemeyer, Wagenmakers, & Stout, 2008) to mathematically model participants' decision-making processes. The model assumes that the evaluation of outcomes follows the prospect utility function, which has diminishing sensitivity to increases in magnitude and loss aversion; that is, different sensitivity to losses versus gains. Specifically, the utility, $u(t)$ on trial t of each net outcome $x(t)$ is expressed as:

$$u(t) = \begin{cases} x(t)^{\alpha} & \text{if } x(t) \geq 0 \\ -\lambda |x(t)|^{\alpha} & \text{if } x(t) < 0 \end{cases}. \quad (1)$$

Here α is a shape parameter ($0 < \alpha < 1$) that governs the shape of the utility function, and λ is a loss aversion parameter ($0 < \lambda < 5$) that determines the sensitivity of losses compared with gains. Net outcomes were scaled for cognitive modeling so that the highest net gain becomes 1 and the largest net loss becomes -11.5 (Busemeyer & Stout, 2002). As α gets close to 1, the utility gets close to the objective outcome amount, and as α gets close to 0, it becomes more like a step function. If an individual has a value of loss aversion (λ) greater than 1, it indicates that the individual is more sensitive to losses than gains. A value of λ less than 1 indicates that the individual is more sensitive to gains than losses.

On the basis of the outcome of the chosen option, the expectancies of decks were updated on each trial using the decay-reinforcement learning rule (Erev & Roth, 1998). When tested with the Bayesian information criterion (Schwarz, 1978), previous studies consistently showed that this rule had the best post hoc model fit (Ahn et al., 2008; Yechiam & Busemeyer, 2005, 2008) compared with others including the delta rule (Rescorla & Wagner, 1972). The decay-reinforcement learning rule assumes that the expectancies of all decks decay (are discounted) with time, and then the expectancy of the chosen deck is added to the current outcome utility:

$$E_j(t) = A \cdot E_j(t - 1) + \delta_j(t) \cdot u(t). \quad (2)$$

The parameter A is a recency parameter ($0 < A < 1$), which determines how much the past expectancy is discounted. $\delta_j(t)$ is a dummy variable that is 1 if deck j is chosen and 0 otherwise.

With the updated expectancies, the softmax choice rule (Luce, 1959) was then used to compute the probability of choosing each deck j. It has a sensitivity (or exploitiveness) parameter, $\theta(t)$, which governs the degree of exploitation versus exploration.

$$Pr[D(t + 1) = j] = \frac{e^{\theta(t) \cdot E_j(t)}}{\sum\limits_{k=1}^{4} e^{\theta(t) \cdot E_k(t)}}. \quad (3)$$

Sensitivity, $\theta(t)$, is assumed to be trial independent and was set to $3^c - 1$ (Ahn et al.,

2008; Yechiam & Ert, 2007). Here c is called *consistency* and was limited from 0 to 5 so that the sensitivity ranges from 0 (*random*) to 242 (*almost deterministic*). In summary, the PVL model used in this study has four free parameters reflecting distinct psychological constructs: A, recency; α, utility shape; c, choice sensitivity; and λ, loss aversion.

Simulation Study

To compare the performance of HBA to the other methods in accurately recovering parameter values, we simulated 30 participants performing the IGT (100 trials per participant) assuming that they behaved according to the PVL model. To be as realistic as possible, we based the simulated data on the actual fMRI study reported in a later section. The number of participants and trials were matched to those of the actual study, and when generating stimulated data, we used parameters estimated from the actual data set. Specifically, the parameters of the simulation agents were the posterior means of the parameters found with HBA for the real participants.[1]

The four free model parameters of each simulated participant were then estimated in four different ways and compared to determine which method recovered the true parameter values most accurately. The four methods are: MLE at the group level (MLE-Group), MLE at the individual level (MLE-Ind), nonhierarchical Bayesian analysis at the individual level (Bayes-Ind), and HBA. HBA yields posterior distributions of the group parameters (HBA-Group) and each individual's parameters (HBA-Ind), so we report them separately. MLE-Group and MLE-Ind are the most widely used approaches in the decision neuroscience field, so we were most interested in comparing estimates from these approaches with those from HBA. The inclusion of Bayes-Ind allowed us to learn something about the degree to which the advantages of HBA were due to the use of

---

[1] We also compared the estimation methods using an independent data set (i.e., randomly generated parameters for simulation agents), and it yielded the same conclusions as reported in the main text. We report the findings using the "nonindependent" data set because the parameters of the simulated agents are more realistic and more likely to be directly comparable with the actual data.

Bayesian estimation versus being due to the use of a hierarchical model.

Parameter Estimation Methods

Maximum likelihood estimation. For MLE-Group, point estimates were made for each parameter that maximized the sum of log-likelihood across all participants (e.g., Daw, O'Doherty, Dayan, Seymour, & Dolan, 2006). We used a combination of grid-search (100 different initial grid positions) and simplex search methods (Nelder & Mead, 1965) implemented in the R programming language (R Development Core Team, 2009).[2] For MLE-Ind, a set of parameters were estimated that maximized the log-likelihood of each individual's one-step-ahead model predictions, again using the combination of grid-search and simplex search methods in R.

Bayesian estimation. For HBA, it is assumed that the parameters of individual participants are generated from parent distributions, which are modeled with independent beta distributions for each parameter:

$$\alpha_i \sim Beta(\mu_\alpha, \sigma_\alpha), \qquad (4)$$

$$\lambda_i^{'} \sim Beta(\mu_\lambda, \sigma_\lambda), \lambda_i = 5 \cdot \lambda_i^{'}, \qquad (5)$$

$$A_i \sim Beta(\mu_A, \sigma_A), \qquad (6)$$

$$c_i^{'} \sim Beta(\mu_c, \sigma_c), c_i = 5 \cdot c_i^{'}. \qquad (7)$$

As implied in these equations, α_i and A_i were limited to values between 0 and 1 and λ_i and c_i were limited to values between 0 and 5. Here μ_z and σ_z are the mean and the standard deviation of the beta distribution of each group-level parameter z (i.e., α, λ, A, and c).[3] The Bayesian method needs the specification of the prior distributions for the parameters, and we used uniform distributions for μ_z and σ_z, which provide flat priors and thus assume no a priori knowledge about these parameters. The range of each μ_z was set between 0 and 1 and each σ_z was set between 0 and $\sqrt{\mu_z(1 - \mu_z)/3}$ so that each distribution was prevented from being bimodal. Different diffuse priors were also tested (e.g., uniform distributions for the beta means and diffuse gamma distributions for their precisions), and they resulted in almost identical

posterior distributions. The hierarchical Bayesian model is represented graphically in Figure 1.

Finally, the observed data matrix from all participants was used to compute the posterior distributions for all parameters according to Bayes rule (Kruschke, 2010). Posterior inference was performed with the Markov chain Monte Carlo (MCMC) sampling scheme in OpenBUGS (Thomas, O'Hara, Ligges, & Sturtz, 2006), an open source version of Win-BUGS (Spiegelhalter, Thomas, Best, & Lunn, 2003), and BRugs, its interface to R (R Development Core Team, 2009). WinBUGS (and OpenBUGS) implements various MCMC computational methods, and it is relatively user friendly and easy to program; thus, it has greatly facilitated Bayesian modeling and its applications (Cowles, 2004). A total of 50,000 samples were drawn after 70,000 burn-in samples with three chains.

For nonhierarchical Bayesian analysis, we again used beta distributions for each participant's parameters. However, no hyper (group) parameters were assumed, and priors of each participant's parameters were uniform beta distributions; for example, $\alpha_i \sim Beta(1,1)$. We used the same number of burn-in samples and real samples as the HBA analyses. For each parameter, the Gelman–Rubin test (Gelman et al., 2004) was conducted to confirm the convergence of the chains. All parameters had $\hat{R}$ values of 1.00 (in most parameters) or, at most, 1.04, which suggested MCMC chains converged to the target posterior distributions. OpenBUGS codes used for all Bayesian analyses are available at http://www.ahnlab.org/home/research/.

Results and Discussion

Figure 2 shows the results of the simulation study focusing on comparisons between HBA-Ind and MLE (MLE-Ind and MLE-Group) methods. Wetzels, Vandekerckhove, Tuerlinckx, and Wagenmakers (2010) showed that

---

[2] See Section 4 of Ahn et al. (2008) for more details.

[3] Typically a beta distribution is denoted by its own α (it is not a shape parameter of the utility function) and β parameters. The mean (μ) of a beta distribution is $\alpha/(\alpha + \beta)$, and the variance (σ^2) is $\alpha\beta/((\alpha + \beta)^2(\alpha + \beta + 1))$; thus, it can be easily shown that $\alpha = \mu[\mu(1 - \mu)/\sigma^2 - 1]$ and $\beta = (1 - \mu)[\mu(1 - \mu)/\sigma^2 - 1]$.
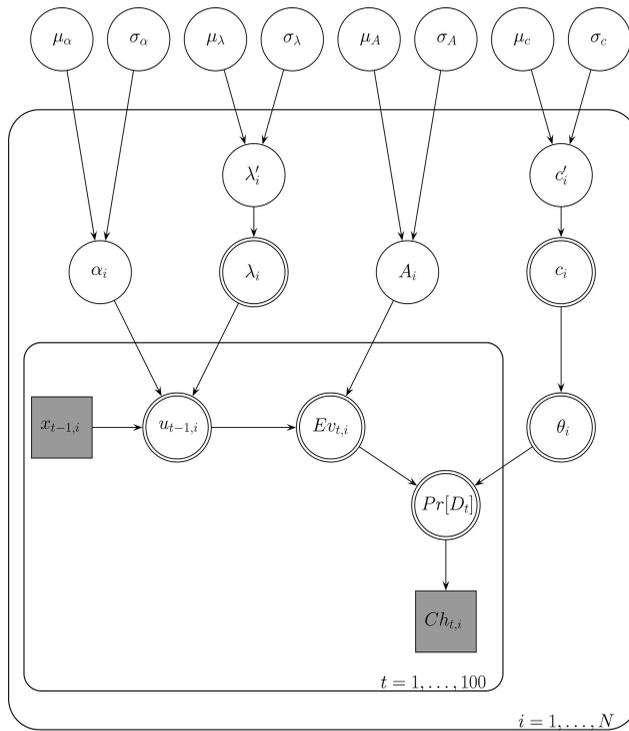
Figure 1.   Graphical depiction of the hierarchical Bayesian analysis for the prospect valence learning model. Clear shapes indicate latent variables; shaded shapes indicate observed variables. Single outlines indicate probabilistic functions of input; double outlines indicate deterministic functions of input. Circles indicate continuous variables; squares indicate discrete variables; rounded rectangular plates indicate replication over the indexing variable. See the main text for a description of the individual parameters.

parameter estimates of an individual's data are not reliable in the expectancy valence learning (EVL) model (Busemeyer & Stout, 2002), which closely resembles the PVL model. However, their claim was based on parameter values estimated with each individual's data only, not all individuals' data in a group. In our data set, parameter estimates of the PVL also show some discrepancy from actual values when using each individual's data only (MLE-Ind in Figure 2). In particular, note that some MLE-Ind estimates are on the parameters' boundary limits, indicating insufficient information in each individual participant's data. However, when estimated with HBA, parameter estimates (HBA-Ind in Figure 2) show much less discrepancy with actual values compared with MLE-Ind estimates.

The HBA results lead to two interesting observations. First, by capturing the dependency between all participants, the HBA estimates regress toward the group mean when there is not much

information in individual participants' data ("shrinkage"; Gelman et al., 2004). Second, HBA can also be sensitive to individual differences when there is enough information, which is demonstrated in the estimates for the learning parameter (*A*). Although the performance of the HBA was not perfect, estimated values from HBA were overall more accurate than those from MLE. Note that we reached the same conclusion when running additional simulations with different true parameter values and different numbers of participants and trials. Regarding MLE-Group estimates, *A* and *c* parameter estimates are around the mean values of individual values, but α and λ estimates are quite different from them.

Figure 3 plots the distribution of posterior means for individual participants' parameter estimates computed from each method (except for HBA-Group, for which distribution densities of group parameters are plotted). When compared
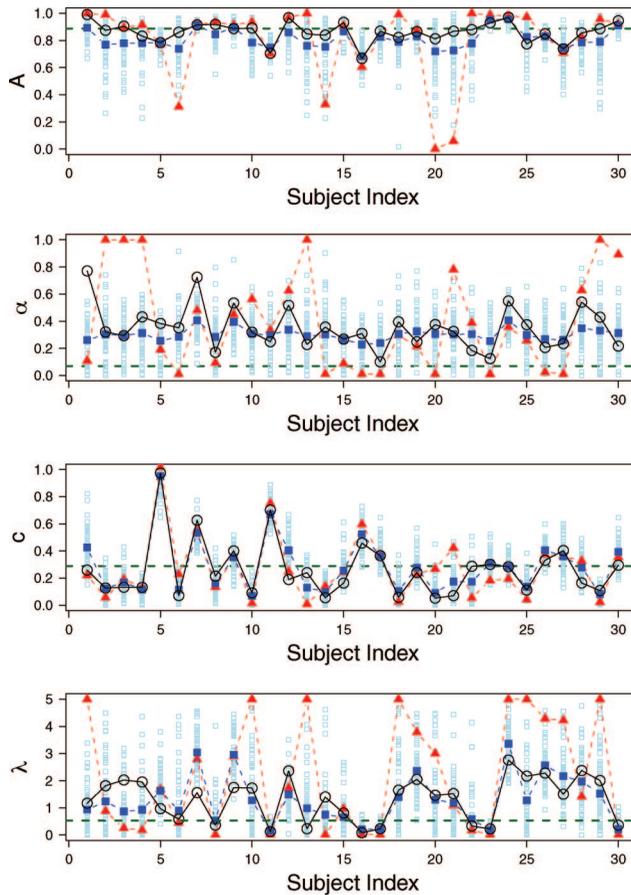
Figure 2.   For the simulation study, parameter estimates of the four free parameters in the prospect valence learning model for each simulated participant from both HBA and MLE. Black circles indicate true parameter values; red triangles indicate MLE-Ind; large blue squares indicate mean HBA-Ind estimates; green horizontal dashed lines indicate MLE-Group estimates; and small sky-blue squares indicate 50 random samples from the posterior distribution of the HBA estimate for each participant. A = recency; α = utility shape; c = choice sensitivity; λ = loss aversion. HBA = hierarchical Bayesian analysis; MLE = maximum likelihood estimation; Ind = individual-level estimates; Group = group-level estimates.

with the true values, the results suggest that HBA performs better than Bayes-Ind and MLE-Ind in recovering true values. The fact that the HBA-Ind estimates are closer to the true values than Bayes-Ind estimates provides empirical support that using a hierarchical approach indeed helps get more accurate estimates.

The posterior distributions of parameters for HBA-Group closely resemble the true parameter distributions. However, these distributions are narrower because they represent the variance in the group estimates, not the variance among individuals.

The results in Figure 3 also give some insight into why the MLE-Group estimates of α and λ are so far from the actual values. The MLE-Group estimates are around the mode of the MLE-Ind distributions. For parameter A, most participants' true values are around the mode, so the MLE-Group estimate looks acceptable. However, for parameters α and λ, the modes of MLE-Ind parameters are near the lower bounds; thus, MLE-Group estimates are dissimilar from the overall patterns of actual values. Note that these results are not because of the estimation method (MLE) but because of the assumption
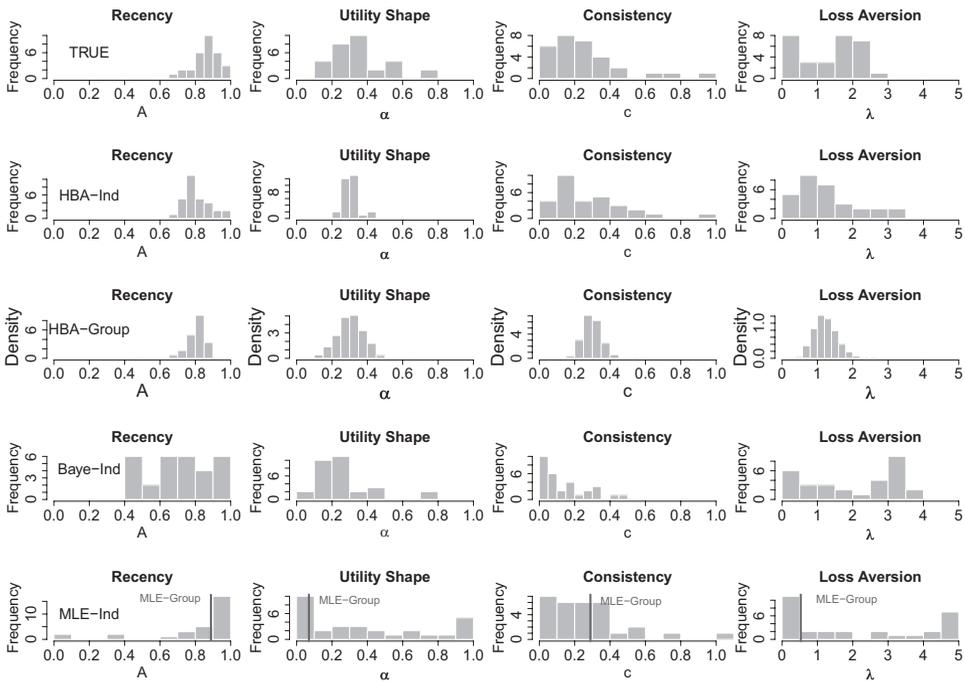
Figure 3. For the simulation study, histograms of the true parameter values and the parameter estimates from each estimation method for all of the simulated participants (except for the third row, which shows the posterior distributions of the group parameters for HBA-Group). HBA = hierarchical Bayesian analysis; MLE = maximum likelihood estimation; Bayes = nonhierarchical Bayesian analysis; Ind = individual-level estimates; Group = group-level estimates.

made in the estimation—namely, that all participants use the same parameter values. Indeed, if the same assumption is used with Bayesian estimation, the posterior means of the parameters are very close to the MLE-Group estimates (for brevity, results are not shown here). In summary, the results of the simulation study suggest that HBA is the best among these methods for estimating free parameters of the PVL model accurately.

Model-Based fMRI Study

Having confirmed the utility of HBA in estimating behavioral parameters, we then wanted to examine how fMRI results would depend on the choice of estimation method. We conducted model-based fMRI analyses of actual data using parameter estimates from three of the estimation methods (HBA, MLE-Ind, and MLE-Group). We included both the individual and group estimates from HBA (HBA-Ind and HBA-Group).

By using group and individual estimates with both MLE and HBA, we could consider the effects of method and analysis level separately. We hypothesized that HBA would yield more power than MLE because its parameter estimates would be more accurate (as revealed by the simulation study) and, thus, its model predictions would better reflect participants' actual cognitive processes. We also predicted that, when MLE-Group and HBA-Group are compared with each other, MLE-Group would yield more power at the second level (group) than the first level (individual), whereas HBA-Group would conversely yield more power at the first level (individual) than the second level (group). This follows from the fact that MLE-Group simply finds a group average parameter, but HBA-Group provides more individualized fits constrained toward the group mean. Regarding comparisons between individual estimates and group estimates, we predicted that MLE-Group would yield more power than MLE-Ind be-

cause, according to the simulation study, MLE-Ind estimates would be noisy and unreliable.

Method

Participants.   We recruited participants from the student body of Indiana University Bloomington. They were required to be at least 18 years of age, to be right handed, and to meet standard health and safety requirements for entry into the MRI scanner. They were paid $25/hr for participation plus performance bonuses based on points earned during the task. A total of 30 participants (mean age = 21.7 years; age range = 18–29; 16 women, 14 men) were used in all reported analyses.

Design and procedure.   Participants performed the IGT for a block of 100 trials.[4] During the task, there were 4 decks of cards labeled A, B, C, and D from left to right. Two of the decks (A and B) are considered bad decks: (Deck A) a net-loss/frequent-loss deck, with 50% loss trials, a mean loss of 25 points per trial, and a gain of 100 on nonloss trials; and (Deck B) a net-loss/rare-loss deck, with 10% loss trials, a mean loss of 25 points per trial, and a gain of 100 on nonloss trials. The other two decks (C and D) are considered good decks: (Deck C) a net-gain/frequent-loss deck, with 50% loss trials, a mean gain of 25 points per trial, and a gain of 50 on nonloss trials; and (Deck D) a net-gain/rare-loss deck, with 10% loss trials, a mean gain of 25 points per trial, and a gain of 50 on nonloss trials. The two bad decks were always adjacent with the frequent-loss deck to the left of the rare-loss deck. The two good decks were also kept adjacent with the frequent-loss deck to the left of the rare-loss deck. The order of the bad and good decks was counterbalanced across participants.

The specific sequences of gains and losses for each deck were the same as in the original task design (Bechara et al., 1994). However, unlike in the original design, each trial outcome was presented as a net gain, draw, or loss; the participant started with an initial sum of 1,000 points; and the entire task was performed on a computer using E-Prime 1.2 (Psychology Software Tools Inc., 2006).

Participants were instructed to select cards from the decks. They were informed that the goal was to maximize earnings and that they would receive a monetary bonus based on the number of points they accumulated. They were informed of the 3 second period in which to make each selection and the running point total at the bottom of the screen. They were told nothing about the order of the decks or how the order might change from block to block.

The timing and presentation of a trial is presented schematically in Figure 4. The participant's running point total was displayed throughout the block at the bottom of the screen. At the start of a trial, a message ("Some decks are better than others") and the 4 decks of cards (labeled A, B, C, and D from left to right) were presented. The participant had 3 s to select a deck by pressing one of their middle or index fingers on buttons corresponding in a spatially compatible way to the decks. If the participant failed to respond within 3 s, then the trial was considered a no-response trial. After the response deadline, there was an exponentially distributed delay of 0, 2, 4, or 6 s. After the variable delay, a card from the chosen deck was flipped over to reveal the outcome as a negative, zero, or positive point value; and the running total was updated. On no-response trials, the outcome was always a loss of 100 points to encourage participants to make a choice on every trial. The feedback remained visible for 0.8 s, after which the message, cards, and outcome were removed for an exponentially distributed intertrial interval of 0.2, 2.2, 4.2, or 6.2 s before the next trial began. The variable-length delays between choice and outcome and between trials were designed to allow the brain activity associated with the decision period to be estimated separately from that associated with response to the outcome (Ollinger, Corbetta, & Shulman, 2001; Ollinger, Shulman, & Corbetta, 2001).

fMRI collection and preprocessing.   Imaging data were collected on a 3.0 Tesla Sie-

---

[4] During fMRI data collection, participants performed the IGT for three blocks of 100 trials each for a larger study that examined the effect of persuasive messages on risky decision making. For each block, a different hint message was presented to the participant. Only data from the blocks with the control message, "Some decks are better than others," were analyzed here. Also, participants whose data sets contained unacceptable spike artifacts were excluded from further analysis. Spike artifacts were due to a technical problem with the scanner and were unrelated to individual participants' anatomy or performance. For the details of the full study, see Krawitz, Fukunaga, and Brown (2010).
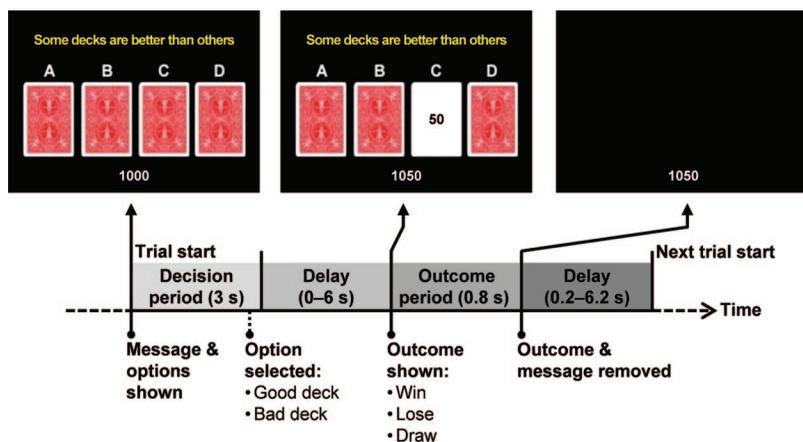
Figure 4. Time course of the Iowa Gambling Task in a rapid event-related functional magnetic resonance imaging design.

mens Magnetom Trio. For each participant, we collected functional BOLD data using echo planar imaging with free induction decay for a block of 360 whole brain volumes with an echo time of 25 ms, a repetition time of 2,000 ms, and a flip angle of 70°. Images were collected in 33 axial slices in interleaved order with 3-mm thickness and 1-mm spacing between slices. Each slice consisted of a 64×64 grid of $3.4375 \times 3.4375 \times 3$-mm voxels. For each participant, we collected a structural scan using three-dimensional TurboFLASH imaging.

We checked each participant's functional volumes for transient spike artifacts in individual slices using a custom algorithm implemented in MATLAB R2007a 7.4.0. Preprocessing of the data was conducted with SPM5 (Wellcome Trust Centre for Neuroimaging, 2005). The raw DICOM images were first converted to NIfTI format. Then we performed slice timing correction on the functional images using SPM5's Fourier phase shift interpolation with the first slice as reference. We then performed motion correction using SPM5's least squares six parameter rigid body transformation. The structural scan was then skull-stripped using BET2 (Péchaud, Jenkinson, & Smith, 2006) with default parameters. The structural scan was then coregistered with the motion-corrected functional scans using SPM5's affine transformation with the mean functional image as reference. We then registered the images for each participant to MNI space using SPM5's

normalization procedure by first performing a 12-parameter affine transformation within a Bayesian framework using regularization to the ICBM space template, followed by a nonlinear deformation using discrete cosine transform basis functions. The source image was the structural scan with an 8-mm Gaussian smoothing kernel, and the template was SPM5's MNI Avg152, T1 at 2 mm^3 along with its associated weighting mask. The resulting normalized images were written with 2-mm^3 voxels. Finally, the normalized images were smoothed with an 8-mm^3 FWHM (full width at half maximum) of the Gaussian kernel.

Model-based fMRI analysis. For model-based fMRI analysis (Daw et al., 2006; McClure et al., 2003; O'Doherty et al., 2004; O'Doherty, et al., 2007; Tanaka et al., 2004), model-generated regressors were convolved with a canonical hemodynamic response function and then correlated against BOLD fMRI signals to determine brain areas related to the specific decision-making processes (using parametric modulation in SPM5). We used choice probability of the chosen option at the time of decision (onset of deck presentation) as the regressor of interest. The choice probability is a relative measure of the expected value signal (Daw et al., 2006). Ventromedial prefrontal cortex (vmPFC) is known to encode reward (Daw et al., 2006; Knutson, Taylor, Kaufman, Peterson, & Glover, 2005), and IGT performance is impaired in vmPFC lesion patients (Bechara et

al., 1994), so we hypothesized that the choice probability computed by the model for the chosen option on each trial would be correlated with activation of vmPFC at the time of decision making.

To increase statistical power, we used summed probabilities for choosing either good or bad decks. In other words, if a good deck was chosen on a given trial, we used the summed probability of choosing either good deck, and if a bad deck was chosen on a trial, we used the summed probability of choosing either bad deck. Analyzing the IGT results in terms of good and bad decks is a common practice (e.g., Bechara et al., 1994; Bechara et al., 1997).

For model-based fMRI with HBA, the regressors were generated directly from the posterior distributions of each participant's parameters (HBA-Ind) or group parameters (HBA-Group), and the means of the posterior predictive distributions were used as input to SPM5.[5] For regressors from MLE, regressors were generated from each participant's point estimates (MLE-Ind) or group point estimates (MLE-Group). In every case, all regressors were standardized into z scores within each participant ($M = 0$, standard deviation $= 1$) before being entered into SPM5.

We performed first-level analysis of the preprocessed fMRI data using SPM5. A general linear model was conducted for each participant with SPM5's canonical hemodynamic response function with no derivatives, a microtime resolution of 16 time-bins per scan, a high-pass filter cutoff at 128 s using a residual forming matrix, autoregressive AR(1) to account for serial correlations, and restricted maximum likelihood for model estimation. The model included a constant term, six motion regressors using the parameters of the motion correction performed during preprocessing, the model-generated regressor, and nuisance regressors. Nuisance regressors included objective outcomes and the absolute value of loss outcomes at the feedback period, reaction times, and onsets of no-response trials (mean number of no-response trials $= 1.8$).

Group-level analyses were conducted with two approaches. The first approach was a whole-brain analysis, which assumes that activations for a given contrast will be in the same location for all participants. This approach used voxel-by-voxel one-sample t tests to test whether the beta coefficients across participants were significantly different from zero. For activation maps in vmPFC, we used a threshold of $p < .001$, uncorrected, with a cluster threshold of 8 contiguous voxels. This approach was selected because it is the most commonly used group-level analysis for model-based fMRI analysis. The second approach was a form of region-of-interest (ROI) analysis where the voxel with peak activation within an a priori ROI is selected for each participant. Our ROI was vmPFC, defined as Brodmann area 25 dilated by 1 mm using the WFU Pick Atlas (Lancaster et al., 2000; Maldjian, Laurienti, Kraft, & Burdette, 2003). We tested the peak values for each participant from this ROI at the second level using an uncorrected one-sample t test. This approach was selected because past work has suggested that the peak voxel best reflects the underlying neural activity (Arthurs & Boniface, 2003), and because this approach allows for individual differences in the particular location of activity.

Results and Discussion

Parameter estimation. Model parameters were estimated from the actual behavioral data with three different methods (HBA, MLE-Ind, and MLE-Group). Table 1 shows the parameter estimates from each method, and Figure 5 illustrates the histograms of parameter estimates from each method. Again, MLE-Ind estimates are often on the boundaries of parameter ranges and MLE-Group estimates of α and λ are near the lower bound of zero. Unlike the simulation study, we do not know true values of these parameters, so we cannot tell which method is the best for estimating them. However, the previous simulation study and other studies (Fridberg et al., 2010; Shiffrin, Lee, Kim, & Wagenmakers, 2008; Wetzels et al., 2010) that examined this issue suggest that the HBA estimates probably better reflect individuals' true internal characteristics.

Model-based fMRI. To focus on the comparison of estimation methods, we limited our fMRI analysis to correlations between choice probability for the chosen option and decision-time activation in the vmPFC. We found such correlations with all four estimation methods

---

[5] Alternatively, regressors can be generated from the means of posterior distributions. For most participants, model-generated choice probabilities were very similar both ways.

Table 1

Comparison of Prospect Valence Learning Model Parameters by Method of Parameter Estimation

Method	A	α	c	λ
μ (HBA-Group)	0.86	0.34	0.29	1.25
Mean of MLE-Ind estimates	0.80	0.48	0.26	2.71
MLE-Group	0.91	0.01	0.25	0.38

Note. Parameter estimates from the 30 participants in the fMRI study. A = recency; $α$ = utility shape; c = choice sensitivity; $λ$ = loss aversion; HBA = hierarchical Bayesian analysis; MLE = maximum likelihood estimation; Ind = individual-level estimates; Group = group-level estimates.

using both approaches to the group-level fMRI analysis. The results from each estimation method and each analysis approach are summarized in Table 2, and the activation maps from the whole-brain analysis are shown in Figure 6. To compare the models in more detail, we plotted z values for all four methods from the whole-brain analysis within a rectangle of MNI space ranging from 0 to 4 in x-coordinates, 10 to 42 in y-coordinates, and -14 to -10 in z-coordinates (see Figure 7). This region includes the vmPFC peak activations found with each of the four methods.

With the whole brain analysis, for HBA and especially MLE, group methods showed higher peak z values and larger regions of activation than individual methods. The MLE-Group method produced the largest vmPFC region correlating with the choice probabilities. The activation maps for HBA-Ind, HBA-Group, and MLE-Ind are quite similar in shape, and their peak coordinates match, but the map for MLE-Group is qualitatively different. The peak of activation is shifted forward along the y-axis for MLE-Group compared with the other methods.

With the ROI analysis, which searches the ROI to find the voxel with the best model fit separately for each individual, the group methods again showed higher peak z values than the individual methods. However, unlike the whole-brain approach, both of the HBA meth-
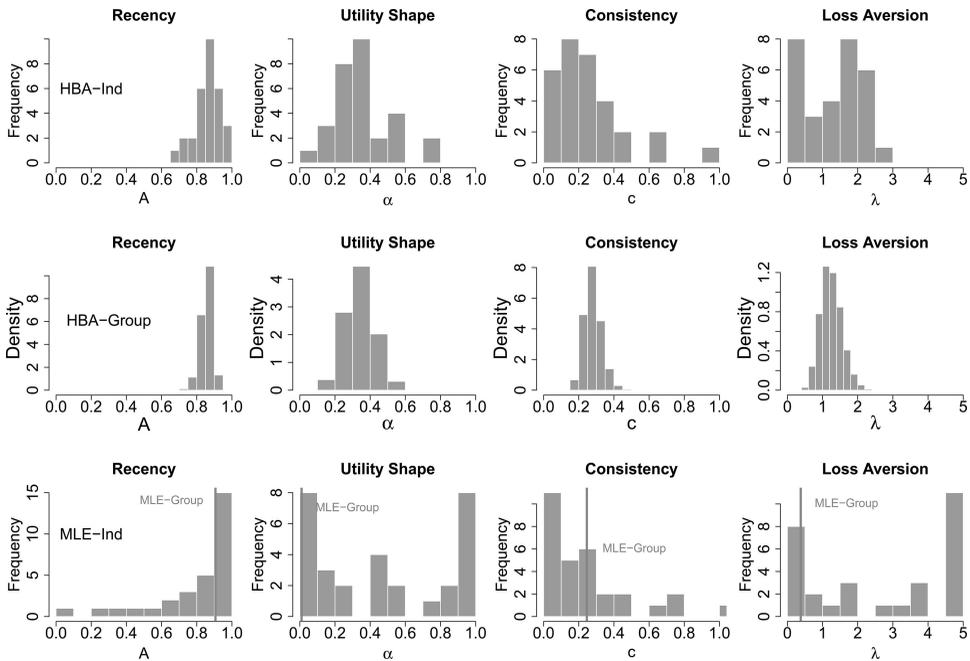

Figure 5. For the model-based fMRI study, histograms of each participant's parameter estimates with each estimation method. Note that the HBA-Ind parameters in the first row were used as the true parameters in the simulation study. HBA = hierarchical Bayesian analysis; MLE = maximum likelihood estimation; Ind = individual-level estimates; Group = group-level estimates.

Table 2
Comparison of PVL Model-Based fMRI Findings by Method of Parameter Estimation and Analysis Approach

	Whole-brain analysis			ROI analysis	
Estimation method	Maximum z value	Cluster size (k_E)	Peak MNI coordinates	Mean peak z value	Mean MNI coordinates
HBA-Ind	3.84	54	[2, 16, −10]	5.20	[0, 12, −14]
HBA-Group	4.17	74	[2, 16, −10]	5.31	[0, 12, −12]
MLE-Ind	3.49	14	[4, 18, −10]	4.99	[0, 12, −14]
MLE-Group	4.41	444	[0, 24, −14]	5.06	[0, 12, −12]

Note. Analysis focused on regions in the ventromedial prefrontal cortex (vmPFC) that correlated significantly with the choice probability for the chosen option assigned by the prospect valence learning (PVL) model. Cluster size is in voxels. ROI = region of interest; HBA = hierarchical Bayesian analysis; MLE = maximum likelihood estimation; Ind = individual-level estimates; Group = group-level estimates.

ods yielded higher z values than either of the MLE methods. Furthermore, the mean locations of the peaks were almost the same for all four methods.

The differences found here between estimation methods in terms of their ability to account for the fMRI data are relatively small. However, it is still interesting to note that to the extent that there are differences, HBA was more successful when the method of analysis allowed for individual differences in the locations of activation. This suggests that, for HBA's advantage in accounting for individual differences in behavior to carry over to the fMRI analysis, that analysis must also allow for individual differences. In addition, HBA-Ind yielded more power than MLE-Ind in both whole brain and ROI analyses, which suggests that allowing some extra parameters in the hierarchical model is helpful in terms of fMRI power when estimating each subject's parameters separately.

What is less clear is why the HBA-Group method outperformed HBA-Ind in the ROI analysis, given that the simulation study suggested that HBA-Ind does the best job of accounting for individual differences in parameter estimates. Further investigation should be conducted to characterize these patterns across a wider range of brain regions, tasks, and model predictions.

General Discussion

The simulation study compared two Bayesian methods (HBA and Bayes-Ind) and two MLE methods (MLE-Ind and MLE-Group) in their performance recovering true parameters and the results suggest that HBA is the best method for obtaining accurate individual and group parameter estimates. Whereas the HBA estimates were close to the true parameter values, the MLE-Ind estimates were often stuck on bounds and some MLE-Group estimates diverged markedly from the true parameter means. Individual estimates from the nonhierarchical Bayesian method (Bayes-Ind) were uninformed by other participants' data and were often too vague and less accurate than HBA estimates.

Subsequent model-based fMRI results were generally consistent with the behavioral results. We predicted that a method that performed well in the stimulation study would yield more significant activations when used for model-based fMRI. We evaluated this prediction in the vmPFC for the correlation of decision-time activity and choice probabilities for the chosen options. As predicted, the HBA-Ind method yielded more vmPFC activation than MLE-Ind, MLE-Group yielded more activation than MLE-Ind, and HBA-Group outperformed MLE-Group in the ROI analysis. However, in the whole-brain analysis MLE-Group yielded the largest vmPFC activation, which was not expected. The best overall performance with respect to power was found with HBA-Group, with the more flexible prior assumption that there may be individual differences in peak voxel location. Nonetheless, when the simplifying assumption was made that there are no individual differences in peak voxel location, then MLE-Group yielded more power than HBA-Group. To our knowledge, this is the first model-based fMRI study with HBA estimation, so further research is needed to confirm and extend the results of this study.
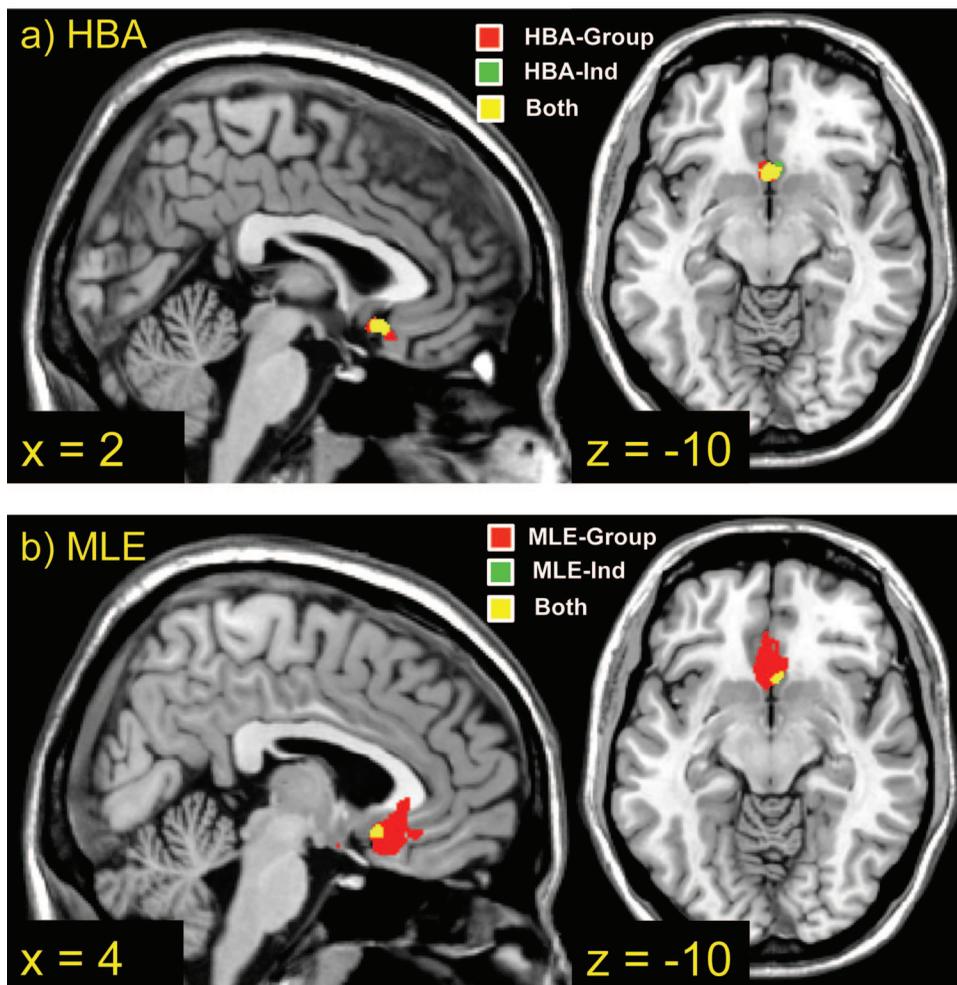
Figure 6. Brain regions whose decision-time activation correlates significantly with the choice probability assigned by the prospect valence learning model using parameter estimates from each estimation method. Thresholded at $p < .001$, uncorrected, cluster size ≥ 8 voxels. HBA = hierarchical Bayesian analysis; MLE = maximum likelihood estimation; Ind = individual-level estimates; Group = group-level estimates.

We demonstrated the use of hierarchical Bayesian parameter estimation with model-based fMRI, and compared this method to other nonhierarchical and non-Bayesian methods. As our results suggest, there may be several advantages to using HBA in studies correlating modeling predictions with both behavior and neural signals. In particular, obtaining more reliable parameter estimates from behavior may in turn better capture individual differences in neural activations underlying the behavior. If participants' data contain enough information, then using nonhierarchical individual-level analysis (MLE-Ind or Bayes-Ind) for model-based fMRI might be sufficient. However, for many real-world scenarios, where only a limited number of trials are collected for each participant, our findings support the use of a hierarchical analysis (e.g., HBA). Although we applied the HBA to model-based fMRI, it can also be used for model-based EEG analysis (Mars et al., 2008) and model-based single-cell monkey electrophysiology analysis. HBA has been recently utilized in many areas including biostatistics,
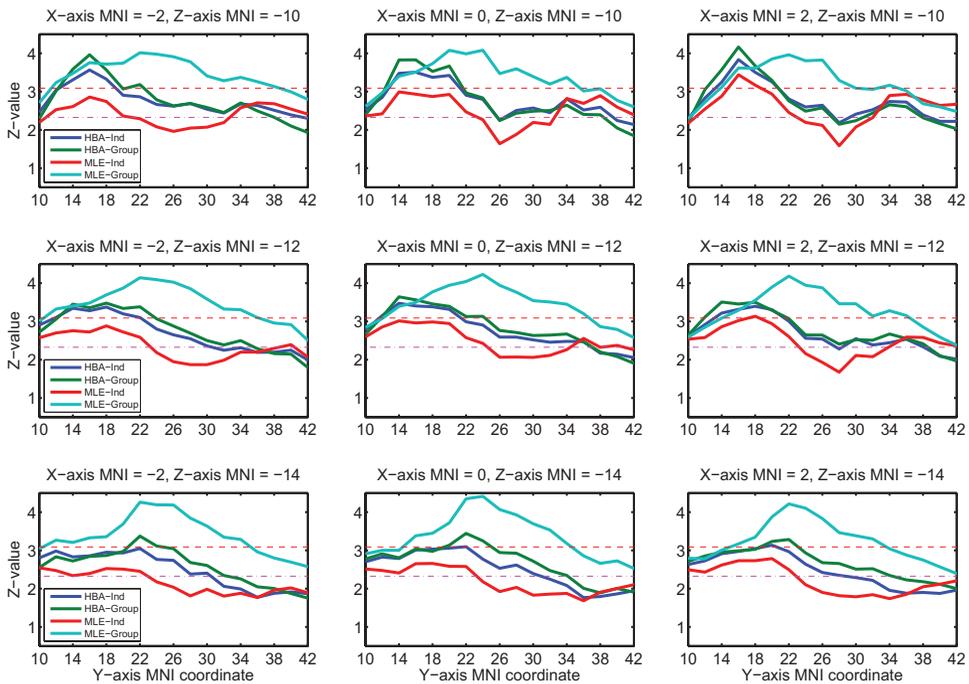
Figure 7. The *z* values as a function of MNI coordinates for decision-time activation correlated with the choice probability assigned by the prospect valence learning model using parameter estimates from each estimation method. Red dashed lines indicate thresholds for $p < .001$ ($z = 3.06$), and purple dashed lines indicate thresholds for $p < .01$ ($z = 2.33$). HBA = hierarchical Bayesian analysis; MLE = maximum likelihood estimation; Ind = individual-level estimates; Group = group-level estimates.

economics, and cognitive modeling and has proven to be a useful method. We believe that it will also be a valuable tool in model-based fMRI and hope that this study will help researchers in decision neuroscience better understand and adopt HBA for their work.

References

Ahn, W.-Y., Busemeyer, J. R., Wagenmakers, E.-J., & Stout, J. C. (2008). Comparison of decision learning models using the generalization criterion method. *Cognitive Science, 32,* 1376–1402.

Arthurs, O. J., & Boniface, S. J. (2003). What aspect of the fMRI BOLD signal best reflects the underlying electrophysiology in human somatosensory cortex? *Clinical Neurophysiology, 114,* 1203–1209.

Bechara, A., Damasio, A. R., Damasio, H., & Anderson, S. W. (1994). Insensitivity to future consequences following damage to human prefrontal cortex. *Cognition, 50,* 7–15.

Bechara, A., Damasio, H., Tranel, D., & Damasio, A. R. (1997). Deciding advantageously before knowing the advantageous strategy. *Science, 275,* 1293–1295.

Bechara, A., Dolan, S., Denburg, N., Hindes, A., Anderson, S. W., & Nathan, P. E. (2001). Decision-making deficits, linked to a dysfunctional ventromedial prefrontal cortex, revealed in alcohol and stimulant abusers. *Neuropsychologia, 39,* 376–389.

Berger, J. O. (1985). *Statistical decision theory and Bayesian analysis.* New York: Springer.

Busemeyer, J. R., & Stout, J. C. (2002). A contribution of cognitive decision models to clinical assessment: Decomposing performance on the Bechara gambling task. *Psychological assessment, 14,* 253–262.

Cowles, M. (2004). Review of WinBUGS 1.4. *The American Statistician, 58,* 330–336.

Daw, N. D., O'Doherty, J. P., Dayan, P., Seymour, B., & Dolan, R. J. (2006). Cortical substrates for exploratory decisions in humans. *Nature, 441,* 876–879.

Erev, I., & Roth, A. (1998). Predicting how people play games: Reinforcement learning in experimental games with unique, mixed strategy equilibria. *American Economic Review, 88,* 848–881.

Fridberg, D. J., Queller, S., Ahn, W.-Y., Kim, W., Bishara, A. J., Busemeyer, J. R., . . . Stout, J. C. (2010). Cognitive mechanisms underlying disadvantageous decision-making in chronic cannabis abusers. *Journal of Mathematical Psychology, 54,* 28–38.

Gelman, A., Carlin, J. B., Stern, H. S., & Rubin, D. B. (2004). *Bayesian data analysis* (2nd ed.). London: Chapman & Hall.

Knutson, B., Taylor, J., Kaufman, M., Peterson, R., & Glover, G. (2005). Distributed neural representation of expected value. *Journal of Neuroscience, 25,* 4806–4812.

Krawitz, A., Fukunaga, R., & Brown, J. W. (2010). Anterior insula activity predicts the influence of positively framed messages on decision making. *Cognitive, Affective, & Behavioral Neuroscience, 10*(3), 392–405.

Kruschke, J. K. (2010). Doing Bayesian Data Analysis: A tutorial with R and BUGS. Academic Press/Elsevier Science.

Lancaster, J. L., Woldorff, M. G., Parsons, L. M., Liotti, M., Freitas, C. S., Rainey, L., . . . Fox, P. T. (2000). Automated Talairach Atlas labels for functional brain mapping. *Human Brain Mapping, 10,* 120–131.

Luce, R. (1959). *Individual choice behavior.* New York:Wiley.

Maldjian, J. A., Laurienti, P. J., Kraft, R. A., & Burdette, J. H. (2003). An automated method for neuroanatomic and cytoarchitectonic atlas-based interrogation of fMRI data sets. *NeuroImage, 19,* 1233–1239.

Mars, R. B., Debener, S., Gladwin, T. E., Harrison, L. M., Haggard, P., Rothwell, J. C., . . . Bestmann, S. (2008). Trial-by-trial fluctuations in the event-related electroencephalogram reflect dynamic changes in the degree of surprise. *Journal of Neuroscience, 28,* 12539–12545.

McClure, S. M., Berns, G. S., & Montague, P. R. (2003). Temporal prediction errors in a passive learning task activate human striatum. *Neuron, 38,* 339–346.

Montague, P. R., Dayan, P., & Sejnowski, T. J. (1996). A framework for mesencephalic dopamine systems based on predictive Hebbian learning. *Journal of Neuroscience, 16,* 1936–1947.

Nelder, J. A., & Mead, R. (1965). A simplex method for function minimization. *Computer Journal, 7,* 308–313.

O'Doherty, J. P., Dayan, P., Friston, K., Critchley, H., & Dolan, R. J. (2003). Temporal difference models and reward-related learning in the human brain. *Neuron, 38,* 329–337.

O'Doherty, J. P., Dayan, P., Schultz, J., Deichmann, R., Friston, K., & Dolan, R. J. (2004). Dissociable roles of ventral and dorsal striatum in instrumental conditioning. *Science, 304,* 452–454.

O'Doherty, J. P., Hampton, A., & Kim, H. (2007). Model-based fMRI and its application to reward learning and decision making. *Annals of the New York Academy of Sciences, 1104,* 35–53.

Ollinger, J. M., Corbetta, M., & Shulman, G. L. (2001). Separating processes within a trial in event-related functional MRI—II. Analysis. *NeuroImage, 13,* 218–229.

Ollinger, J. M., Shulman, G. L., & Corbetta, M. (2001). Separating processes within a trial in event-related functional MRI—I. The method. *NeuroImage, 13,* 210–217.

Péchaud, M., Jenkinson, M., & Smith, S. (2006). *Brain extraction tool (BET).* Oxford, England: Oxford University Centre for Functional MRI of the Brain.

Psychology Software Tools Inc. (2006). *E-Prime.* Pittsburgh, PA: Author.

R Development Core Team. (2009). *R: A language and environment for statistical computing.* Vienna: R Foundation for Statistical Computing.

Rescorla, R., & Wagner, A. (1972). *A theory of Pavlovian conditioning: Classical conditioning, II.* New York: Appleton-Century-Crofts.

Schultz, W., Dayan, P., & Montague, P. R. (1997). A neural substrate of prediction and reward. *Science, 275,* 1593–1599.

Schwarz, G. (1978). Estimating the dimension of a model. *The annals of statistics,* 461–464.

Shiffrin, R., Lee, M., Kim, W., & Wagenmakers, E. (2008). A survey of model evaluation approaches with a tutorial on hierarchical Bayesian methods. *Cognitive Science: A Multidisciplinary Journal, 32,* 1248–1284.

Spiegelhalter, D., Thomas, A., Best, N., & Lunn, D. (2003). *WinBUGS version 1.4 user manual.* Cambridge, United Kingdom: MRC Biostatistics Unit.

Tanaka, S. C., Doya, K., Okada, G., Ueda, K., Okamoto, Y., & Yamawaki, S. (2004). Prediction of immediate and future rewards differently recruits cortico-basal ganglia loops. *Nature Neuroscience, 7,* 887–893.

Thomas, A., O'Hara, B., Ligges, U., & Sturtz, S. (2006). Making BUGS Open. *R News, 6,* 12–17.

Wellcome Trust Centre for Neuroimaging. (2005). *Statistical parametric mapping (SPM).* London: Author.

Wetzels, R., Vandekerckhove, J., Tuerlinckx, F., & Wagenmakers, E. (2010). Bayesian parameter estimation in the expectancy valence model of the Iowa gambling task. *Journal of Mathematical Psychology, 54,* 14–27.

Yechiam, E., & Busemeyer, J. R. (2005). Comparison of basic assumptions embedded in learning models for experience-based decision making. *Psychonomic Bulletin & Review, 12,* 387–402.

Yechiam, E., & Busemeyer, J. R. (2008). Evaluating generalizability and parameter consistency in learning models. *Games and Economic Behavior, 63,* 370–394.

Yechiam, E., & Ert, E. (2007). Evaluating the reliance on past choices in adaptive learning models. *Journal of Mathematical Psychology, 51,* 75–84.